

1  
2  
3  
4  
5  
6  
7  
8  
9  
10  
11  
12  
13  
14  
15  
16  
17  
18  
19  
20  
21  
22

# **Early *C. elegans* embryos modulate cell division timing to compensate for, and survive, the discordant conditions of a severe temperature gradient**

Eric Terry<sup>1,2</sup>, Bilge Birsoy<sup>1</sup>, David Bothman<sup>2</sup>, Marin Sigurdson<sup>2</sup>, Pradeep M. Joshi<sup>1</sup>, Carl  
Meinhart<sup>2</sup>, and Joel H. Rothman<sup>1,\*</sup>

1. Department of MCD Biology and Neuroscience Research Institute, University of  
California Santa Barbara, CA, USA 93106

2. Department of Mechanical Engineering, University of California Santa Barbara, CA,  
USA 93106

\*Corresponding author: Joel H. Rothman

Email: [joel.rothman@lifesci.ucsb.edu](mailto:joel.rothman@lifesci.ucsb.edu)

## 23 **Abstract**

24 Despite a constant barrage of intrinsic and environmental noise, embryogenesis is  
25 remarkably reliable, suggesting the existence of systems that ensure faithful execution of  
26 this complex process. We report that early *C. elegans* embryos, which normally show a  
27 highly reproducible lineage and cellular geometry, can compensate for deviations  
28 imposed by the discordant conditions of a steep temperature gradient generated in a  
29 microfluidic device starting at the two-cell stage. Embryos can survive a gradient of up to  
30 7.5°C across the 50-micron axis through at least three rounds of division. This response  
31 is orientation-dependent: survival is higher when the normally faster-dividing anterior  
32 daughter of the zygote, AB, but not its sister, the posterior P<sub>1</sub>, is warmer. We find that  
33 temperature-dependent cellular division rates in the early embryo can be effectively  
34 modeled by a modification of the Arrhenius equation. Further, both cells respond to the  
35 gradient by dramatically reducing division rates compared to the predicted rates for the  
36 temperature experienced by the cell even though the temperature extremes are well  
37 within the range for normal development. This finding suggests that embryos may sense  
38 discordance and slow development in response. We found that in the cohort of surviving  
39 embryos, the cell on the warmer side at the two-cell stage shows a greater average  
40 decrease in expected division rate than that on the cooler side, thereby preserving the  
41 normal cellular geometry of the embryo under the discordant conditions. A diminished  
42 average slow-down response correlated with lethality, presumably owing to disruption of  
43 normal division order and developmental fidelity. Remarkably, some inviable embryos in  
44 which the canonical division order was reversed nonetheless proceeded through  
45 relatively normal morphogenesis, suggesting a subsequent compensation mechanism

46 independent of cell division control. These findings provide evidence for a previously  
47 unrecognized process in *C. elegans* embryos that may serve to compensate for  
48 deviations imposed by aberrant environmental conditions, thereby resulting in a high-  
49 fidelity output.

50

51

## 52 **Introduction**

53           The development of a complex multicellular animal from a zygote requires  
54 coordination of diverse biological processes. Each step in the process is associated with  
55 a particular rate of error and is subject to perturbation by genetic variation, environmental  
56 fluctuations, and intrinsic molecular noise [1]. Nonetheless, despite the incessant  
57 onslaught of error-provoking influences, development generally proceeds faithfully in  
58 organisms spanning metazoan phylogeny [2–8]. The observed rate of success is  
59 remarkable: throughout the complex process of embryogenesis, cells must properly  
60 satisfy many parameters of identity and behavior, including appropriate gene expression,  
61 incidence and timing of cell division, and spatiotemporal positioning. This ability of  
62 development to proceed with high fidelity in the face of environmental and intrinsic  
63 variation likely reflects evolutionary selection for robustness-conferring cellular and  
64 molecular mechanisms [1].

65           While the processes that regulate spatiotemporal developmental fidelity have not  
66 been comprehensively elucidated, several mechanisms that influence developmental  
67 precision have been uncovered. The molecular chaperone, Hsp90, has been found to act  
68 as a buffer against cryptic variation in both fly and vertebrate models [9–14], helping to  
69 ensure appropriate cellular identity during development. Robustness in spatial  
70 coordination is exemplified by transformation of a variable Bicoid gradient along the  
71 antero-posterior axis of the *Drosophila* embryo into spatially stereotyped expression  
72 pattern of hunchback and ultimately cellular identity along the anterior-posterior axis of  
73 developing embryos [3,15,16]. In vertebrates, Notch directs intercellular temporal  
74 coordination and precision during somite development [17] and mutations in the Notch

75 signaling pathway result in the loss of the normal synchrony in division oscillations of  
76 somite cells [17–19]. While such findings shed light on processes that regulate  
77 developmental precision, systems that mediate developmental fidelity, particularly in the  
78 temporal dimension, are not well understood.

79         The early cell divisions in *C. elegans* embryos establish six “founder cell” lineages.  
80 While the founder cells are born by a series of asynchronous divisions, all their  
81 descendants divide in approximate synchrony with a cell cycle periodicity that is unique  
82 to that lineage [20]. Although the different founder cell division clocks are not  
83 synchronized with each other, they must be kept in precise register to ensure the highly  
84 stereotyped arrangement of cells that is characteristic of early embryogenesis [20,21].  
85 This reproducible geometry is critical for signaling events that depend on the proper  
86 spatial arrangements of cell-cell contacts that are essential for normal development to  
87 proceed [22,23].

88         The differential apportionment of cell division clocks is evident as early as the two-  
89 cell stage, in which the larger, anterior daughter of the zygote, the AB blastomere, divides  
90 before its posterior sister, P<sub>1</sub>, with high precision. This difference in cell cycle timing is  
91 passed onto the descendants of each cell, such that the cell cycle periodicity in the AB  
92 lineage is shorter than in the P<sub>1</sub> lineage. The regulation of this differential timing control  
93 system has been thought to be determined by cell-autonomous mechanisms; when  
94 isolated AB and P<sub>1</sub> are allowed to develop in culture, the relative division timing difference  
95 is largely preserved [20,24–28]. The difference in the cell cycle clocks of AB and P<sub>1</sub> largely  
96 correlates with their different molecular content and size [25,29,30], which are controlled

97 by the machinery that establishes anteroposterior polarity in the zygote following  
98 fertilization [31–33].

99         The high fidelity of molecular processes such as DNA replication and aminoacyl-  
100 tRNA charging [34,35] result from reactions that correct errors after they are made and it  
101 is conceivable that errors made in embryogenesis are often corrected through  
102 subsequent developmental processes. Indeed, development is characterized by  
103 substantial plasticity and regulatory mechanisms often generate precise patterning from  
104 more disordered assemblages of cells (e.g. ordered patterning of hair follicles [36] and  
105 robust patterning by morphogen gradients [37–43]). When cells in different domains of  
106 *Drosophila* embryos are forced to develop at different rates by imposition of a temperature  
107 (T) gradient, abnormal patterns of cell divisions arise (with fewer nuclei on the colder  
108 side); however, developmental gene expression is resolved into normal patterns along  
109 the axis [44,45], revealing that the gene expression patterning machinery can correct for  
110 abnormal cellular patterns that were induced by discordant conditions occurring earlier in  
111 development.

112         The highly stereotypical division sequence and arrangement of early blastomeres  
113 in the rapidly developing *C. elegans* embryo [20,21,24,46,47] persists across  
114 developmental rates that vary over nearly an order of magnitude (dependent on the T of  
115 the environment), providing a useful system for probing mechanisms that ensure  
116 developmental precision and fidelity. How are the founder cell lineages, each with  
117 different cell cycle clocks, coordinated irrespective of developmental rate, environmental  
118 variation, and intrinsic molecular noise, ensuring a reproducible outcome? It is  
119 conceivable that communication between cells in different lineages functions to tune cell

120 division timings while they are occurring, thereby continuously maintaining proper  
121 harmony across the developing embryo. Alternatively, deviations might be compensated  
122 by subsequent error-correcting responses that renormalizes cellular geometry.

123 If early *C. elegans* embryos harbor mechanisms that correct for environmental  
124 variation, then they may undergo stereotypical development even under the discordant  
125 conditions imposed by a T gradient that, in the absence of such correction, would drive  
126 cell divisions and placements to deviate from the normal pattern.

127 In this study, we investigated whether developing *C. elegans* embryos can  
128 compensate and correct for discordant conditions between lineages by subjecting them  
129 to steep T gradients along the long (anteroposterior) axis. To achieve this, we designed,  
130 fabricated, and validated a novel microfluidic device that establishes a steep T gradient  
131 in which the two extremes are nonetheless within the permissive T ranges for normal  
132 development. While embryos in this steep gradient would be predicted to undergo out-of-  
133 sequence division patterns and die in the absence of correction, remarkably, we found  
134 that embryos can survive a T gradient of up to 7.5°C across the 50-micron axis through  
135 at least three rounds of division from first cleavage, suggesting that they can compensate  
136 for the large discordance imposed by the gradient. This response showed orientation-  
137 dependence: survival was higher when the normally faster-dividing anterior daughter of  
138 the zygote, AB, but not its posterior sister, P<sub>1</sub>, was at the warmer T. We found that the  
139 division timing of both AB and P<sub>1</sub> slowed down dramatically in the presence of the gradient  
140 compared to the predicted rates, suggesting that embryos may sense and respond to the  
141 “crisis” of a discordant condition by activating a checkpoint-like system. Further, cells on  
142 the warmer side slow by a larger extent relative to predicted rates than cells on the cooler

143 side, with the result that the normal division sequence and geometry are preserved. The  
144 magnitude of this response correlated with embryo survival: those with a stronger “tuning”  
145 response (adjustment in division rate) showed a higher tendency to survive, whereas  
146 those with a modest response generally died, suggesting that the response ensures  
147 normal developmental progression. In the largest T gradient, the canonical division  
148 sequence of many embryos was reversed, with a warmer P<sub>1</sub> dividing ahead of AB.  
149 Although such embryos invariably died, some nonetheless showed signs of relatively  
150 normal morphogenesis, suggesting a later compensation mechanism can act  
151 independently of cell division control. These findings are consistent with the possibility  
152 that early *C. elegans* embryos possess mechanisms that sense and correct for noise-  
153 induced variation at the time it occurs and respond by adjusting cell division rates to  
154 restore the normal pattern of development.



155 **Results**

156 **Development and validation of a microfluidics T gradient device**

157 We sought to investigate whether early *C. elegans* embryos are capable of  
158 responding to, and correcting for, severely discordant environmental conditions by  
159 subjecting them to a steep T gradient across their long axis. We posit that if no  
160 compensation system exists, this environmental discordance would drive opposite ends  
161 of the embryo to develop at different rates. Based on the known relationship between  
162 development timing and T[48], a gradient of 5°C across the 50 µm anteroposterior axis  
163 would be expected to create an ~1.5x difference in the developmental rates of P<sub>1</sub> and AB  
164 in the absence of any adjustments made by the embryo. To perform this test for  
165 developmental compensation, we designed and fabricated a microfluidic device (Fig. 1;  
166 Movie S1; see Materials and Methods) that establishes a gradient of up to 7.5°C across  
167 the long axis of the developing embryo, while ensuring that the cells within the embryo  
168 remained within permissive, non-stressful Ts for normal development (between 16°C and  
169 24°C).

170 The microfabricated device that generated the T gradient used a platinum Joule  
171 micro-heater to establish the high T side of the gradient and a chilled fluid mixture to cool  
172 the surface opposite from that containing the heater. The magnitude of the T gradient was  
173 controlled by varying the T of the cooling fluid and the power through the Joule heater.  
174 Embryos were flowed into the device through microchannels with a syringe pump and  
175 properly oriented and trapped between pillars in the microfluidic device (Fig. 1E, F; Movie  
176 S2).

177 Computational model and numerical simulations predicted that the device would  
178 effectively generate the desired magnitude of T gradient. We experimentally validated the  
179 actual T profile of the device by filling the microchannels through which embryos were  
180 delivered with a T-dependent fluorophore, dextran-conjugated rhodamine B (DCRB), and  
181 measuring the relative quantum yield (Fig. 2B, C). The measured T profile closely  
182 matched that of the modeled distribution (Fig. 2B, D). We modeled heat transfer through  
183 the eggshell and cytoplasm to assess whether the T gradient experienced by the embryo  
184 is likely to diverge substantially from the measured environment in the channel (see  
185 Materials and Methods). Using even extremely conservative parameters, neither the  
186 eggshell, nor fluid convection, reduce the T-gradient in the embryo by more than a few  
187 percent, hence the device effectively generates a pole-to-pole difference in T experienced  
188 by the embryo of up to 7.5°C.

### 189 **Embryonic survival is dependent on orientation and magnitude of the T gradient**

190 *C. elegans* embryos develop successfully over a broad T range of 6°C to 26°C. At  
191 uniform T, the rate of development and cell division increases by ~50% for every 5°C  
192 increase in T [48]. If cells in a T gradient divide at the rate predicted from the average T  
193 experienced and the embryo is unable to correct for this discordance, the division  
194 sequence would be expected to diverge substantially from the normal pattern. At the two-  
195 cell stage, for example, this could reverse the normal division order, in which the AB cell  
196 divides before the P<sub>1</sub> cell. Such out-of-sequence divisions would be expected to result in  
197 aberrant arrangements of cells that diverge substantially from the normally highly  
198 stereotyped pattern. Given the rapid intercellular signaling events in the early embryo that  
199 are essential for normal cell specification and position [22,29,32,33,49,50] and that

200 depend upon precise alignment of signaling and receiving cells, such derangement of the  
201 pattern would be expected to lead to defective embryogenesis, as evidenced by a failure  
202 to hatch. Thus, we asked whether discordance imposed by the steep T gradient results  
203 in aberrant cell division and geometry and consequent lethality.

204 We performed an initial assessment to determine whether 1-4-cell stage embryos  
205 can survive in a T gradient by loading them into an early version of the device in which  
206 the magnitude of the T gradient differed depending on the position of the captured embryo  
207 in the device (Fig. 3). This approach allowed us to evaluate hatching as a function of  
208 different gradient magnitudes without changing experimental parameters. A flow rate of  
209 at least 25 nl/min was essential for adequate oxygen and CO<sub>2</sub> exchange required to keep  
210 embryos viable in the microfluidic device even in absence of a gradient (Fig. 3A). The  
211 embryos were subjected to an optimal flow rate of 500 nl/min, which is 20x the critical  
212 flow rate necessary for viability without altering the T gradient profile of the microfluidic  
213 device (see supplemental text). Early embryos were subjected to the T gradient for ~1  
214 hour, unloaded from the device, allowed to develop, and scored the following day for  
215 hatching on culture plates. We found that the embryos were frequently able to survive  
216 through to hatching into viable L1 larvae after exposure to the gradient during the crucial  
217 early periods of development. The survival (hatching) rate showed an approximately  
218 monotonic decrease with increasing magnitude of the gradient (Fig. 3B). While all  
219 embryos survived exposure to a 2°C gradient (n=9), ~50% survived in a pole-to-pole T  
220 gradient of 2.5-3°C (n=20) and ~25% survived as the magnitude of the gradient was  
221 increased from 3°C to 5.5°C (n=46). Under these conditions, none of the embryos  
222 exposed to a 6°C T differential hatched (n=5). These initial observations revealed that a)

223 early exposure of *C. elegans* embryos to a T gradient results in significant lethality, b) the  
224 degree of lethality correlates with the magnitude of the gradient, and c) some embryos  
225 can survive even in very substantial gradient of  $\sim 5.5^{\circ}\text{C}$  along the long axis.

226 To observe individual divisions and characterize the survival of one and two-cell  
227 embryos subjected to the gradient as a function of number of divisions, we loaded  
228 embryos into a modified device before the division of the first cell, and after the division  
229 of the first cell. This allowed us to measure the times of division for each cell while in the  
230 gradient. Embryos were loaded into the device in either orientation such that, for some,  
231 AB was on the warmer end of the gradient (positioned toward the heater), and for others,  
232 P<sub>1</sub> was warmer. Embryos were allowed to develop in the gradient through the division of  
233 the daughters of AB and P<sub>1</sub>, unloaded, allowed to develop at constant T, and scored for  
234 hatching  $\sim 24$  hours later. Confirming the results with the earlier device, we found that  
235 embryos were frequently able to survive a large T gradient (Fig. 3C). The hatching rate  
236 of embryos subjected to the gradient starting at the two-cell stage again correlated  
237 roughly monotonically with magnitude of the T gradient. Remarkably, we found that some  
238 embryos were able survive a very steep pole-to-pole gradient of  $7^{\circ}\text{C}$ .

239 We observed that the ability of early embryos to survive exposure to the gradient  
240 was orientation-dependent. Embryos that were placed in the gradient such that AB was  
241 warmer than P<sub>1</sub> showed a statistically significantly higher (65.8%; n=38) rate of hatching  
242 when compared to embryos with the opposite orientation (P<sub>1</sub> warmer than AB) (28.6%  
243 n=42; p=0.0015 Fisher exact test). Above the threshold of a  $5^{\circ}\text{C}$  gradient, survivability in  
244 both orientations started to drop, with P<sub>1</sub> warmer embryos experiencing a significantly  
245 larger drop in survival (Fig. 3C). At the highest magnitude of gradient ( $7^{\circ}\text{C}$ ), while nearly

246 a quarter of the embryos survived when AB was oriented toward the warm end of the  
247 gradient (n=18), all embryos (n=17) in the reverse orientation died, a significant difference  
248 (p=0.045). These results raise the possibility that the more rapidly dividing AB cell can  
249 more effectively “tune” its division rate in response to discordance than the slower dividing  
250 P<sub>1</sub> cell, consistent with our observations of cell cycle timing adjustment (see below).

### 251 **Early rates of division described with a modified Arrhenius equation**

252 We sought to test the possibility that the ability of embryos to survive a T gradient  
253 might reflect a system that monitors deviations in the early cell division and then adjusts  
254 cell division timings to normalize these deviations. To do so, it was necessary to quantify  
255 the T-dependent behavior of the cells at uniform constant T<sub>s</sub>, and assess whether cells  
256 divide at rates that differ from those predicted for their T environment under the discordant  
257 conditions of the gradient. If the two-cell *C. elegans* embryo adjusts cell division timings  
258 based on this discordance, this effect would be revealed as a tendency for one or both of  
259 the cells to divide at a rate other than that expected for the T experienced by that cell. To  
260 reveal any such an effect, it was necessary to measure the division rates for AB and P<sub>1</sub>  
261 at a range of constant T<sub>s</sub>, and build a quantitative mathematical model of the division time  
262 for the second and third divisions in the AB and P<sub>1</sub> lineages as a function of T (Fig. 4A &  
263 B).

264 We found that the T-dependent times of division for both cells in the two-cell  
265 embryo measured at progressively increasing constant T are empirically closely  
266 described by a modified Arrhenius equation. This finding is consistent with those  
267 described by Begasse et al. [51] for T-dependent rates of pre-division events observed in  
268 the one-cell P<sub>0</sub> zygote in both *C. elegans* and *C. briggsae*. In that study, as in ours, the

269 data was modeled by performing a least-squares fit to a linearized version of the  
270 Arrhenius equation in which the log of the rate (or time interval) of an event is evaluated  
271 as a function of the reciprocal of T at which the rate (or time to division) was measured.  
272 However, and significantly, our model differs from the previous work in at least one  
273 important aspect. The earlier work [51] used the absolute T scale of Kelvin to describe  
274 the relationship between rate and T. While this is consistent with calculation of T-  
275 dependent chemical rates using the Arrhenius equation, it makes the assumption that the  
276 event under consideration progresses at some rate down to a T approaching absolute  
277 zero. However, such an assumption does not hold for typical biological processes. In an  
278 alternative method introduced by Nakamura et al. [52], an additional T term is introduced  
279 into the denominator of the independent variable of the linear form of the Arrhenius  
280 equation, allowing for greater empirical fitting of data:

281 
$$\ln(\Gamma_1 - \Gamma_0) = B\left(\frac{1}{T - T_0}\right) + \ln A$$

282 This additional term, which acts as an offset for the measured T of the data, can be  
283 thought of as the T at which of the rate for the system under consideration extrapolates  
284 to zero. We sought an estimate for this T for *C. elegans* by performing two methods of  
285 analysis on our data: a numerical-simulation-generated general non-linear fit of the data,  
286 performed in Comsol Multiphysics, and a parametric sweep of this offset T on the linear  
287 model of the data. Both methods were in high agreement (~one part in 100 difference)  
288 and revealed that the offset T that best fits our data for the N2 strain of *C. elegans* for the  
289 second and third division of the embryo is -10°C. This parameter implies a *C. elegans*-  
290 specific “absolute zero” T, at which all cellular activity stops, a more biologically relevant  
291 assumption.

292

293 **Embryos respond to a T gradient by slowing overall developmental rate**

294 Our modified Arrhenius equation allowed us to calculate an expected rate of cell  
295 division at any T within the experimental T ranges and to assess whether the individual  
296 cells divided at a rate consistent with, or deviating from, the local T that they experience  
297 in the gradient. We followed cell division microscopically throughout exposure to the  
298 gradient and quantified the temporal division behavior of each of the cells in the two-cell  
299 embryo. This analysis revealed two striking trends in the quantitative behavior of the  
300 individual cells within the gradient (Fig. 4C-H).

301 First, we found that the timing of cell divisions in the gradient showed much greater  
302 variability than that observed for embryos at constant T. To compare the variance of  
303 cohorts of embryos across the various conditions, we calculated the coefficient of  
304 variation (CV) for each cohort of embryos at each of the constant Ts, as well as the CV  
305 of each cohort of embryos that experienced the same T gradient magnitude and  
306 orientation. The mean coefficient of variation across constant Ts for both AB and P<sub>1</sub> were  
307 0.10, and the standard deviation of the CVs across the different constant Ts were 0.05  
308 and 0.04 respectively. The mean CV of the various cohorts of embryos experiencing the  
309 T gradient was 0.19 and 0.18 for AB and P<sub>1</sub> respectively with a standard deviation of CVs  
310 across gradients and orientations of 0.06 and 0.04 for AB and P<sub>1</sub> respectively. That the  
311 standard deviation of the CVs stayed relatively constant across both constant Ts and T  
312 gradient conditions and orientations, while the magnitude of the CV doubled for the  
313 various T gradient conditions when compare to the constant T divisions, implies that the  
314 presence in the gradient imposes greater variability in division timing.

315           Second, we found that the division rates of both cells, independent of the  
316 orientation of the embryos in the gradient, decrease in the T gradient relative to their  
317 expected T-dependent behavior at their local T. This effect suggests that embryos  
318 respond to the discordant conditions by reducing the overall rate of development.  
319 Regardless of the mechanism underlying this process, many embryos showing this  
320 greatly reduced developmental rate survived, revealing their ability to adjust to these  
321 highly aberrant conditions (Fig. 3 and see below). There were two exceptions to the  
322 general trend of slowing relative to the rate expected for T environment. First, for embryos  
323 that experienced a T gradient of 5°C starting at the 1-cell stage, the division rates were  
324 more consistent with the expected behavior for the local T (Fig. 4I and J). Moreover, the  
325 rate of division of P<sub>1</sub> in embryos exposed to the largest gradient (Fig. 4H) similarly  
326 deviated less dramatically from the expected behavior. In both cases, embryos in the  
327 cohorts that tracked more closely with expected timing were much more likely to die, a  
328 trend that we observed more generally as well (see below).

329

330 **On average, the warmer cell slows more than the cooler cell in viable embryos**  
331 **irrespective of orientation**

332           While imposition of the T gradient slowed the division rate of both AB and P<sub>1</sub>, it  
333 was possible that a compensation process that normalizes the division sequence might  
334 occur in which one cell is subject to greater reduction in division rate than the other,  
335 depending on orientation in the gradient. To assess the extent to which the cell division  
336 rate was altered, we analyzed the division timing of each cell (AB and P<sub>1</sub>) relative to the  
337 other. For each embryo analyzed, we determined the fold change in division timing for



338 each of the cells of the two-cell embryo by calculating the  $\log_2$  of the ratio of observed  
339 and expected time of division at the average T experienced by each cell. The behavior of  
340 each embryo was then graphed as a single point, with the behavior of AB plotted on the  
341 x axis and P<sub>1</sub> on the y axis (Fig. 5). This treatment allowed us to simultaneously identify  
342 how each cell behaved relative to both its expected behavior and to that of the other cell,  
343 as explained in Fig. 5A. The results allowed us to compare the deviations in  
344 developmental timing of each cell relative to the other in the context of the entire embryo  
345 with those measured in embryos developing at constant T. Consistent with the high fidelity  
346 of early *C. elegans* development, we found that embryos at constant T showed low  
347 variation in cell division rates around the origin of both axes [ $\log_2$  (expected: observed) =  
348 ~0]. If division timings of both cells slowed by the same magnitude relative their expected  
349 timings, the results would fall on a line with slope = 1, and the distance from the origin  
350 along this line would reflect the overall slow-down as a result of the gradient. Divergence  
351 from this line indicates that the division rate of one of the two cells deviated from the  
352 expected division rate by a larger extent than the other cell.

353 The data were partitioned into four groups. Results for embryos in each orientation  
354 (AB warmer vs. P<sub>1</sub> warmer) were averaged and plotted separately. Further, to assess  
355 whether the degree of deviation in cell division timing might correlate with successful  
356 embryogenesis in the discordant conditions, the results were further separated based on  
357 the ultimate outcome (viability vs. lethality) following exposure to the gradient.

358 This analysis revealed a striking outcome: embryos that developed and hatched  
359 (i.e., were viable) showed a substantially larger average overall reduction in division  
360 timing from that expected at constant T (greater distance from the origin) compared to the

361 cohort of embryos that failed to hatch (i.e., were lethal) (Fig. 5C). Thus, survival correlated  
362 with greater slow-down in division rates of both AB and P<sub>1</sub>, irrespective of orientation in  
363 the gradient.

364 For the cohort of embryos that survived, we found that the two cells showed a  
365 pronounced orientation-dependent difference. For viable embryos positioned in the  
366 gradient with P<sub>1</sub> on the warmer end, the slow-down in average division rate from the  
367 expected rate was greater for P<sub>1</sub> than for AB. Similarly, viable embryos in which AB  
368 experienced the warmer environment showed a greater reduction in average division rate  
369 of AB compared to P<sub>1</sub> (Fig. 5C). These results suggest that, for surviving embryos, while  
370 the division of both cells slowed dramatically in the T gradient, the cell on the warmer side  
371 tended to respond to the discordance to a greater degree relative to the T it experienced  
372 than that on the cooler side, with the outcome that normal division sequence was  
373 preserved.

374 We observed a second orientation-dependent effect: viable embryos in which P<sub>1</sub>  
375 was warmer (P<sub>1warm</sub>) than AB experienced a greater magnitude in slowdown of P<sub>1</sub> relative  
376 to the extent of slowdown of AB in the viable AB<sub>warm</sub> embryos. Regardless, in both cases,  
377 the cell on the warmer side of the gradient always showed greater deviation from the  
378 expected rate. AB, the faster dividing cell under normal conditions, appears to be more  
379 effective at responding to the discordance than P<sub>1</sub>, the normally slower developing cell, a  
380 finding that is consistent with the orientation-dependent effect on lethality described  
381 above (Fig. 5C).

382 In contrast to the results with viable embryos, the cohorts of inviable embryos  
383 tended to show a substantially reduced average response of both AB and P<sub>1</sub>: in both

384 orientations, the data clustered closer to the origin than for the viable embryos. Moreover,  
385 unlike the surviving embryos, these inviable embryos showed a greater reduction in  
386 division rate of AB compared to  $P_1$  in *both* orientations, with the result that the data for  
387 the two orientations clustered together (Fig. 5C).

388 In summary, we found that both AB and  $P_1$  greatly reduce their division rates in  
389 embryos that survive the T gradient and that the cell that would be expected to divide  
390 more rapidly on the basis of its higher T environment shows a larger response (greater  
391 reduction in division rate) than its cooler neighbor.

392

393 **Evidence for a later compensation mechanism: morphogenesis can progress**  
394 **despite reversal in the AB and  $P_1$  division sequence**

395 Under the most extreme conditions, we found that the T gradient was sufficient to  
396 force reversal of the stereotyped division sequence of AB and  $P_1$  (Fig. 6). For embryos  
397 subjected to the gradient after cleavage of  $P_0$  and oriented with  $P_1$  on the warmer side,  
398 we found that a steep T gradient was sufficient to reverse the normal division sequence  
399 and drive  $P_1$  to divide before AB in 60% (9/15) of embryos subjected to a 6.5°C gradient,  
400 and 71% (12/15) of those experiencing a 7°C gradient. Further, initiation of the gradient  
401 prior to the division of  $P_0$ , in which the posterior side of the embryo was oriented toward  
402 the warmer end of gradient, resulted in reversal of the division sequence in 90% (9/10) of  
403 the embryos. As expected, none of these embryos in which the sequence of division was  
404 reversed survived and hatched. Unexpectedly, however, a substantial fraction of such  
405 embryos proceeded through relatively normal morphogenesis: 32% (9/28) of embryos  
406 that experienced a reversal in division sequence of AB and  $P_1$  gave rise to an arrested

407 embryo that appeared relatively normal in morphology and had undergone substantially  
408 normal morphogenesis (Fig. 6). Moreover, we found that 43% (6/14) of lethal embryos  
409 that experienced any of the gradients in which AB was warmer than P<sub>1</sub>, similarly  
410 proceeded through relatively normal morphogenesis. These findings revealed that even  
411 under extremely discordant conditions that drive complete reversal of the stereotyped  
412 division sequence in the very early embryo, later embryos appear to be capable of  
413 compensating sufficiently well that morphogenesis, if not fully successful development,  
414 can occur. These observations underscore the substantial ability of *C. elegans* to correct  
415 for aberrations in cell division and placement patterns.

416

417 **Discussion**

418

419 A largely unexplored problem in animal biology is how complex developmental  
420 processes result in a reliable output in spite of constant environmental and intrinsic noise.  
421 Our goal in this study was to test whether animal embryos that normally show a highly  
422 stereotyped pattern of development are capable of responding to, and correcting for, the  
423 discordant conditions imposed by a T gradient. We propose that this discordance is a  
424 proxy for natural noise that embryos normally experience which, in the absence of any  
425 correction, might otherwise cause them to deviate from the stereotypical pattern. These  
426 studies demonstrated that *C. elegans* embryos both respond to a T gradient and can  
427 adjust division timings to generate a normal pattern of development despite highly  
428 discordant T's.

429 In this study, we report the following major findings. 1) We have designed,  
430 fabricated, and validated a microfluidics device that effectively establishes a steep T  
431 gradient of up to 7.5°C across the 50 µm anteroposterior axis of *C. elegans* embryos. 2)  
432 We have characterized the division time of the two-cell embryo as a function of T and  
433 established a mathematical model describing the relationship. 3) Embryos through at  
434 least the second round of division can survive exposure to a pole-to-pole gradient of up  
435 to 7°C and hatch into viable larvae. 4) Survival in the T gradient is orientation-dependent:  
436 embryos in which AB is positioned on the warmer side can withstand a larger gradient  
437 than those in the reverse orientation. 5) Embryos exposed to the T gradient slow their  
438 average developmental rate dramatically compared to those embryos that do not survive  
439 to hatching at the same gradient magnitude. 6) While the rate of division of both cells at  
440 the two-cell stage is reduced in the gradient, the cell on the warmer end shows a tendency

441 to slow by a larger degree than that on the cooler end, thereby often preserving the normal  
442 geometry of the embryo. 7) Survival correlates with the magnitude of this cell division  
443 response: the cohort of embryos that died showed a lower average deviation in division  
444 timing from that predicted based on their T environment. 8) Some embryos in which the  
445 AB/P<sub>1</sub> division sequence was reversed invariably died but nonetheless showed signs of  
446 relatively normal morphogenesis, suggesting the existence of later developmental  
447 compensation mechanisms.

448

#### 449 **Evidence for multiple compensation/correction systems in embryos**

450 Mechanisms that detect and correct for “errors” resulting from noisy development  
451 processes might function by (A) sensing deviations in rates or timing of events outside  
452 normal bounds and adjusting for these deviations at the time of their occurrence, or (B)  
453 by acting at pre-established stages (perhaps “checkpoints”) to detect aberrant events that  
454 have occurred in the past, and make repairs through subsequent compensation  
455 processes. Our findings are consistent with both types of systems in *C. elegans* embryos.

456 The finding that the division of both cells slows in the gradient relative to the  
457 expected behavior is consistent with the possibility that the discrepancy from normal  
458 development imposed by the gradient activates a checkpoint-like system in which a  
459 “crisis” leads to slowing or pausing of the cell cycle (as occurs, for example, in genotoxic-  
460 induced stress [29,53–55]). This effect correlates with survival: the cohort of embryos that  
461 survived showed the most dramatic reduction in developmental rate. We postulate two  
462 possible explanations for this effect. First, it is conceivable that T gradient across each  
463 cell induces a cell-intrinsic process that slows the rate of division in response to the

464 aberrant environment independently of effects on the other cell. A second possibility is  
465 that such a response might result from intercellular communication between AB and P<sub>1</sub>  
466 that instructs both cells to slow or “wait” until adjustments to division rates have been  
467 made. In such an event, this cell-extrinsic communication would be bidirectional, as both  
468 cells slow down relative to their expected behaviors. Thus, each cell at this, and possible  
469 later stages, might compare its progress with neighboring cells and “tune” its division  
470 timing in such a way that the proper geometry is ensured. Resolution of these alternatives  
471 would require creating a step-gradient in which two sharply delineated T’s are imposed  
472 upon the cells, where each T is experienced uniformly across the full dimension of the  
473 cell. If the effect we have observed also occurs under such conditions, it would strongly  
474 argue that the effect is mediated through cell-extrinsic signaling.

475         We found that as early as the two-cell stage, embryos show evidence of “tuning”  
476 of cell divisions in response to deviations: under conditions in which each cell would be  
477 expected to divide at an inappropriate time relative to the other, AB and P<sub>1</sub> often appear  
478 to adjust their division rates in a way that maintains their normal relative division  
479 sequence. It is therefore conceivable that a cell that might be driven to divide more rapidly  
480 as a result of a warmer T might alter its division rate based on information about the rate  
481 of its cooler neighbor. Our results suggest that when its cooler neighbor is lagging, AB  
482 shows a greater capability for slowing its division than does P<sub>1</sub>. This is reflected both in  
483 the magnitude of the division rate decrease (Fig. 5) and the higher viability of embryos in  
484 which AB is located on the warm side than those in reverse orientation. Given that AB is  
485 the “leader” during normal development (i.e., it divides before P<sub>1</sub> under constant T  
486 conditions), this may reflect the intrinsic ability of AB under normal conditions to monitor

487 and respond to its slower neighbor as needed to maintain the proper relative division  
488 timing. Regardless, if AB and P<sub>1</sub> undergo intercellular communication to regulate  
489 developmental progress, it could explain the observation that isolated AB blastomeres,  
490 obtained by removal of P<sub>1</sub> by extrusion from the eggshell or through isolation in culture,  
491 undergo slower rates of division ([27,56,57]; our unpublished observations); in the  
492 absence of information from P<sub>1</sub> that might indicate progress in its development, AB may  
493 default to a slower division rate. Our findings also raise the question of whether the  
494 adjustment in cell division timing observed here is related to a different cell timing  
495 compensation mechanism: the negative correlation between cycle timing of a cell and its  
496 descendant, in which cells that divide early give rise to granddaughters that are more  
497 likely to divide late [46].

498 Our observations suggest that the capacity of embryos to compensate for the  
499 discordance of the T gradient can be exceeded beyond an acceptable “dynamic range”  
500 under extreme conditions. Most or all embryos fail to complete normal embryogenesis  
501 when exposed to the largest gradient (Figs. 3 and 5). We note that under these extreme  
502 conditions, the magnitude of the overall slowdown relative to the expected rate is less  
503 than under milder T gradient conditions, suggesting that the response system may be  
504 overwhelmed by this environment. It is also striking that the cohort of surviving embryos  
505 show the greatest average reduction in both overall cell division rate and in relative  
506 slowdown of the warmer vs. colder cells: in the viable embryos the warmer cell division  
507 rate slowed down related to its expected rate by a larger factor than that of the cooler cell,  
508 hence restoring what would have otherwise been an out-of-sequence division pattern.  
509 Thus, it appears that the embryos that respond most dramatically and correct the



510 discordance most effectively are the most likely to survive. We propose that this effect  
511 may reflect an active process that corrects for noise-induced drift and ensures a faithful  
512 output.

513 Our data also support the existence of a later-acting compensatory system that  
514 correct errors after the early cell divisions. Although some “P<sub>1</sub>-warm” embryos failed to  
515 correct for the discordant conditions and reversed the stereotyped division sequence,  
516 they could nonetheless proceed through apparently relatively normal development,  
517 resulting in a worm-like, albeit lethal, animal (Fig. 6). Rapid signaling events in the early  
518 embryo depend on precise geometry of cells (for example, in the induction of both gut in  
519 the EMS lineage and of ABp-specific fate by the P<sub>2</sub> cell; [22,58–64]). Our observations  
520 suggest that morphogenesis can be coordinated and corrections made even after an  
521 embryo with aberrant cellular arrangements has formed. This finding is consistent with  
522 reports that, at elevated T's, much later mid-stage embryos show variability in cell  
523 positions and cell lineage patterns and yet resolve into normal healthy animals through  
524 normal cell repositioning and morphogenesis [21,65,66].

525

### 526 **Potential regulatory processes in compensation to discordance**

527 It will be of interest to understand the molecular machinery that might mediate the  
528 profound cell division timing adjustments we have observed in embryos exposed to the T  
529 gradient. The asynchrony of AB and P<sub>1</sub> division timing is known to reflect at least two  
530 checkpoint-based regulatory systems. First, cell-size-dependent control by ATL-1 and  
531 CHK-1 accounts for approximately 40% of the difference in cell cycle timing between AB  
532 and P<sub>1</sub> [29]. The other system acts independently of cell size and depends on localization

533 of PLK-1 and CDC-25.1 in P<sub>1</sub> [67,68]. The tight regulation of the cell cycle seen in early  
534 in *C. elegans* embryogenesis is also apparent in mice, in which DNA damage and spindle  
535 assembly checkpoints are active [69,70]; however, this does not appear to be the case in  
536 other vertebrates, including *Xenopus* and zebrafish [71,72], in which these cell division  
537 regulatory systems are enabled only after the midblastula transition. It is conceivable that  
538 regulatory events that influence either the ATL-1/CHK-1 checkpoint system or the PLK-1  
539 checkpoint system in the early *C. elegans* embryo could mediate the response to  
540 discordant conditions of the T gradient.

541 A prominent example of a system that coordinates cellular timing during  
542 development, thereby ensuring highly reproducible patterning, is the segmentation clock  
543 for somitogenesis in vertebrate embryos, which is controlled in part by Notch signaling  
544 [17–19,73]. Notch signaling is also used to specify cell identities throughout development  
545 in *C. elegans*, including in the very early embryo [22,74]. It is intriguing to note that the  
546 maternally provided GLP-1 Notch receptor is differentially expressed as early as the two-  
547 cell stage in *C. elegans*, where it is translated in AB but not P<sub>1</sub>. Moreover, LIN-12, the  
548 other Notch receptor, is zygotically expressed as early as the 24-cell stage [75] and its  
549 (presumably maternal) transcript has been detected at low levels as early as the one-cell  
550 stage [76,77]. While it is tempting to speculate that Notch signaling might function in  
551 coordination of AB and P<sub>1</sub> division, no Notch ligand has been found to be expressed as  
552 early as the two-cell stage, though the APX-1 ligand is expressed, and functions, in its  
553 daughter P<sub>2</sub>; [63]. It will be of interest to test whether early embryos lacking both Notch  
554 receptors show an altered response to a T gradient, in which case Notch signaling might

555 be implicated in mediating communication between AB and P<sub>1</sub> that coordinates their  
556 division timing.

557

### 558 **Other potential implications of compensation to a T gradient**

559 Our findings may be relevant to understanding the factors that dictate the T limits  
560 over which poikilotherms are able to develop successfully. It is generally accepted that  
561 these limits reflect, in part, the T range over which critical intracellular components are  
562 able to function properly. Studies of closely related species of nematodes and flies  
563 demonstrate that there is a uniform scaling of development in time as a function of T  
564 [51,78]. The exponential nature of the T-dependent rates of events in the one-cell *C.*  
565 *elegans* embryo [51], and the T-dependent model of the first cell divisions described here,  
566 raise the possibility that the failure of development at T's that are just outside the range  
567 for successful development might also be the result of divergence of cell division clocks  
568 within the developing animal as a result of a breakdown in the compensation system.

569 Finally, the apparent compensatory system suggested by these findings may  
570 account for observations that human embryos are particularly susceptible to failure early  
571 during embryogenesis, which appears to be coupled with mismatches in cellular timing in  
572 very early embryonic cells [79]. An early-acting system that detects and compensates for  
573 cell-cycle timing defects might function as a global developmental abort system in higher  
574 organisms, particularly when full-term development is costly.

575

## 576 **Materials and Methods**

### 577 **Construction of a microfluidic device to generate a stable steep T gradient.**

578         The microfluidic device consists of two main layers: a backplane, containing the  
579         vias and electrodes of the device and a second layer of microchannels placed on top of  
580         the backplane (see supplemental text for detailed method). The device uses a platinum  
581         Joule micro-heater to establish the high T side of the gradient. The Joule heater along  
582         with four micro resistive thermal devices (RTDs) acting as local T sensors, are  
583         simultaneously patterned through micro-lithography and metal deposition on a glass  
584         substrate. Electrical current generates an approximate cylindrical dispersal of heat around  
585         and away from the Joule heater. To reject the heat and focus the T gradient, a chilled  
586         fluid mixture is flowed underneath and in contact with the glass substrate on the surface  
587         opposite from that containing the heater. The magnitude of the T gradient as well as its  
588         rate of change is controlled by varying the T of the fluid underneath the glass, as well as  
589         the power through the Joule heater. A microfluidic channel with “trapping pillars” to  
590         capture and orient *a C. elegans* embryo within the T gradient, is placed on top of the  
591         heater. The microfluidic channel terminates at the end of the glass substrate where  
592         microbore tubing is affixed in a manner that allows embryos to be introduced into the  
593         device.

594

### 595 **Characterization of the in-device T gradient**

596         The T gradients generated in the microfluidic device were characterized using  
597         thermometric microscopy to correlate the fluorescence intensity of Rhodamine B with T  
598         and measurements from on board resistive thermal sensors or devices (RTDs). After

599 ensuring that there are no bubbles in the microchannels, the water was replaced by a  
600 dilute solution of dextran conjugated Rhodamine B (DCRB). To construct a standard  
601 curve relating T at each point in the channels with fluorescence intensity, approximately  
602 30-60 fluorescence images of the DCRB filled microchannels are taken at each T  
603 between 30°C and 1.5°C which is achieved by regulating the voltage applied to the Joule  
604 heater. The T at each point in the device is estimated by the classical least squares model  
605 for each pixel. 2D Finite element analysis was performed using Comsol Multiphysics  
606 versions 5.1-5.2a. Built-in material properties were used, with the notable exceptions of  
607 the physical parameters for SU-8, and NOA 81, which were both estimated to have the  
608 physical properties of polyethylene. Cooling fluid flow under the device was assumed to  
609 be laminar. The resistance measured by the different RTDs in the gradient was correlated  
610 with the T using standard least squares fitting (see supplemental text).

611

## 612 **Embryo preparation and loading**

613 Embryo experiments were conducted with the *C. elegans* laboratory reference  
614 strain N2 which was maintained as described by Stiernagle [80]. Strains were maintained  
615 at either room T (18-22°C) or in a 15°C incubator. Young adult worms are cut open under  
616 a dissecting scope in osmotically balanced Edgars egg salts solution as described by  
617 Edgar and McGhee [59] and selected embryos are transferred via mouth pipette to the  
618 end of tubing that is connected to the inlet ports of the microfluidic device. One-cell  
619 embryos were loaded into the device either before pronuclear meeting or immediately  
620 after. For two-cell embryos, we continued to track development outside of the microfluidic  
621 device until the first membrane cleavage, at which point they were loaded into the device,

622 using a syringe pump. Embryos generally reached the capture region of the device within  
623 30-60 seconds. A flow of 500nl/min was maintained in the device while embryos were in  
624 the device to ensure that they did not experience hypoxic conditions. Embryos were  
625 unloaded from the device by operating the syringe in reverse. The embryos were then  
626 transferred with a mouth pipette to a standard agar plate seeded with E. coli OP50 and  
627 incubated at room T and scored if they hatched or were dead ~ 24 hours later. Embryos  
628 with reversed sequence of cell division were observed 24 hours later on a Nikon Eclipse  
629 Ti at 100X magnification

630

### 631 **Estimation of cell division rate**

632 Embryos were imaged on an upright Nikon Microphot microscope at 10 second  
633 intervals. Cell division interval was determined as time between successive cytokinesis  
634 as inferred by the first image that shows apparent completion of membrane pinching. For  
635 embryos loaded after the first division, the rate of division was estimated using the  
636 measured room T and the linear model of time of division as a function of T.

637

### 638 **Acknowledgements**

639 Nematode strains used in this work were provided by the Caenorhabditis Genetics  
640 Center, which is funded by the National Institutes of Health - Office of Research  
641 Infrastructure Programs (P40 OD010440). This work was supported by grants from NIH  
642 (#1 R21 HD075292).

643

644 **Figure legends**

645

646 **Figure 1. Microfluidic device design.** A) The two-cell *C. elegans* embryo is subjected  
647 to a T gradient. Normally, in absence of a gradient under constant uniform Ts, AB divides  
648 before P<sub>1</sub>. In a gradient AB and P<sub>1</sub> divide with rates of division determined by the T  
649 experienced by the respective cell. In absence of a coordination mechanism between the  
650 two cells (left), it is possible to establish a T differential at which the order of division of  
651 AB and P<sub>1</sub> is reversed wherein the warmer P<sub>1</sub> cell divides before the cooler AB cell. If  
652 there were a coordination mechanism (right) that corrects for the discordant conditions,  
653 the embryo should resist the T-dependent rates of division allowing for the canonical order  
654 of AB and P<sub>1</sub> divisions. B) Microfluidic device used to capture and orient embryo in a T  
655 gradient. In the example shown here the embryo is oriented such that the posterior  
656 smaller P<sub>1</sub> blastomere is closer to the heating element and experiences a warmer T while  
657 the larger anterior AB blastomere experiences a cooler T. C-F) Schematic of the layout  
658 of device at four scales. C) Macro view of the device. Blue indicates channels, orange  
659 indicates T sensors (RTD) and magenta indicates a Joule heater. D) Closer view of T  
660 sensing regions of RTDs and capture region. E) View showing all three channels, capture  
661 regions for embryos in each channel, Joule heater, and RTDs close to Joule heater. F)  
662 Closeup of a single capture region and example of embryo size and placement. Spacing  
663 between heater and lower RTDs is 10µm. Width of the heater and RTDs is 10µm

664

665 **Figure 2. Characterization of the T gradient in the microfluidic device.**

666 Characterization and modeling of the T gradient in the microfluidic device using Dextran

667 conjugated Rhodamine B (DCRB). A) Yellow circle represents the pixel intensities of  
668 DCRB analyzed. B) (Left) Linear model relating fluorescence intensity of DCRB to T and  
669 (right) 97.5% confidence interval distance from model for the inverse linear model of  
670 intensity to T, as function of T. C) False coloring heat map of T distribution in device during  
671 operation. D) Black data points and error bars indicate the average Ts and standard error  
672 across all three channels as a function of position in the channel. X=0 indicates the center  
673 of the Joule heating element. Blue line is the model estimate of Ts along the interior  
674 bottom of the microfluidic device. Black line is the model estimate of the depth average T  
675 in the channel and Orange line is the model estimate of T in the embryo. Blue dots  
676 correspond to RTD T measurements at the position relative to the heater

677

678 **Figure 3. Survival in the T gradient is dependent on both the magnitude of the**  
679 **gradient and orientation of the embryo.** A) Fraction of embryos completing  
680 development in the microfluidic channel. B) Survival of mixed stage early embryos (1- 4  
681 cells) after ~ 1 hour in the device and then unloaded and placed on agar plates to  
682 complete development. C) Survival of embryos in gradients of different magnitudes.  
683 Pooled data for embryos in both orientations, embryos with anterior (AB) warm, and  
684 embryos with posterior (P<sub>1</sub>) warm in T gradients of different magnitudes are shown. The  
685 rightmost graph represents embryos loaded prior to first cell division in a 5°C T gradient  
686 (Fisher exact test p<0.05 \*\*p<0.01 \*\*\*p<0.001)

687

688 **Figure 4. Cell division rates of individual blastomeres in the T gradient.** Linear model  
689 of division time of AB (A) and P<sub>1</sub> (B) as a function of T. Notched box plots are data at



690 various  $T_s$ . Innermost line indicates linear model. Next outer pair of lines indicate 95%  
691 confidence interval while the outermost pair of lines indicate 95% prediction interval. C-  
692 H) Notched box plot of division time for AB (left) and  $P_1$  (right) at the corresponding T  
693 plotted over the corresponding model. In both AB and  $P_1$  plots, the left box corresponds  
694 to when the cell is close to the heater and the right box corresponds to when the cell is  
695 away from the heater. This cohort of embryos were loaded after formation of first  
696 cleavage. I and J) same as C-H except these embryos were loaded in a 5°C gradient  
697 before the first cleavage.

698

699 **Figure 5. Analysis of deviations in division rates of AB and  $P_1$ .** A) Explanatory graph  
700 for fold change in division time for whole embryo. B) Scatter plot for whole embryo  
701 behavior when (left)  $P_1$  is warm and (right) AB is warm. Black data points represent  
702 embryos that did not survive to hatching while blue and red represent those that did.  
703 Crosses and error bars are mean and SE. C) Mean, SE, and 95% CI for fold changes in  
704 AB and  $P_1$ , based on orientation and survival. Blue-embryos with  $P_1$  warmer than AB,  
705 Red-embryos with AB warmer than  $P_1$ . Black standard error bars identify populations that  
706 did not survive. Colored ellipses represent two-dimensional 95%CI for each population.  
707 The black data point at origin and the surrounding gray ellipse are the mean and 95%CI  
708 respectively of control embryos at a uniform T.

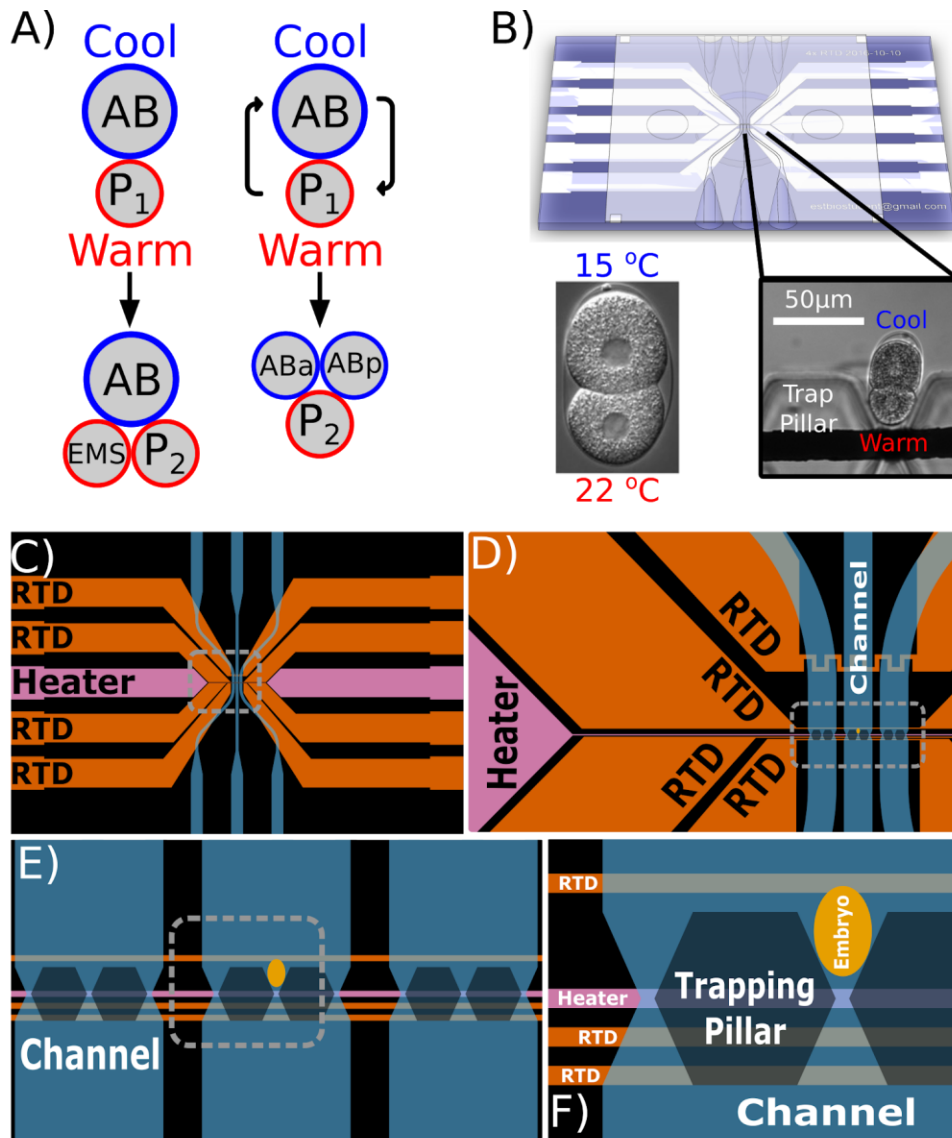
709

710 **Figure 6. Relatively normal morphogenesis following out of sequence divisions of**  
711 **AB and  $P_1$ .** Time lapse images and outline of early cell divisions of AB and  $P_1$ . Top panel:  
712 stereotyped control embryos with the larger anterior AB cell dividing before the smaller

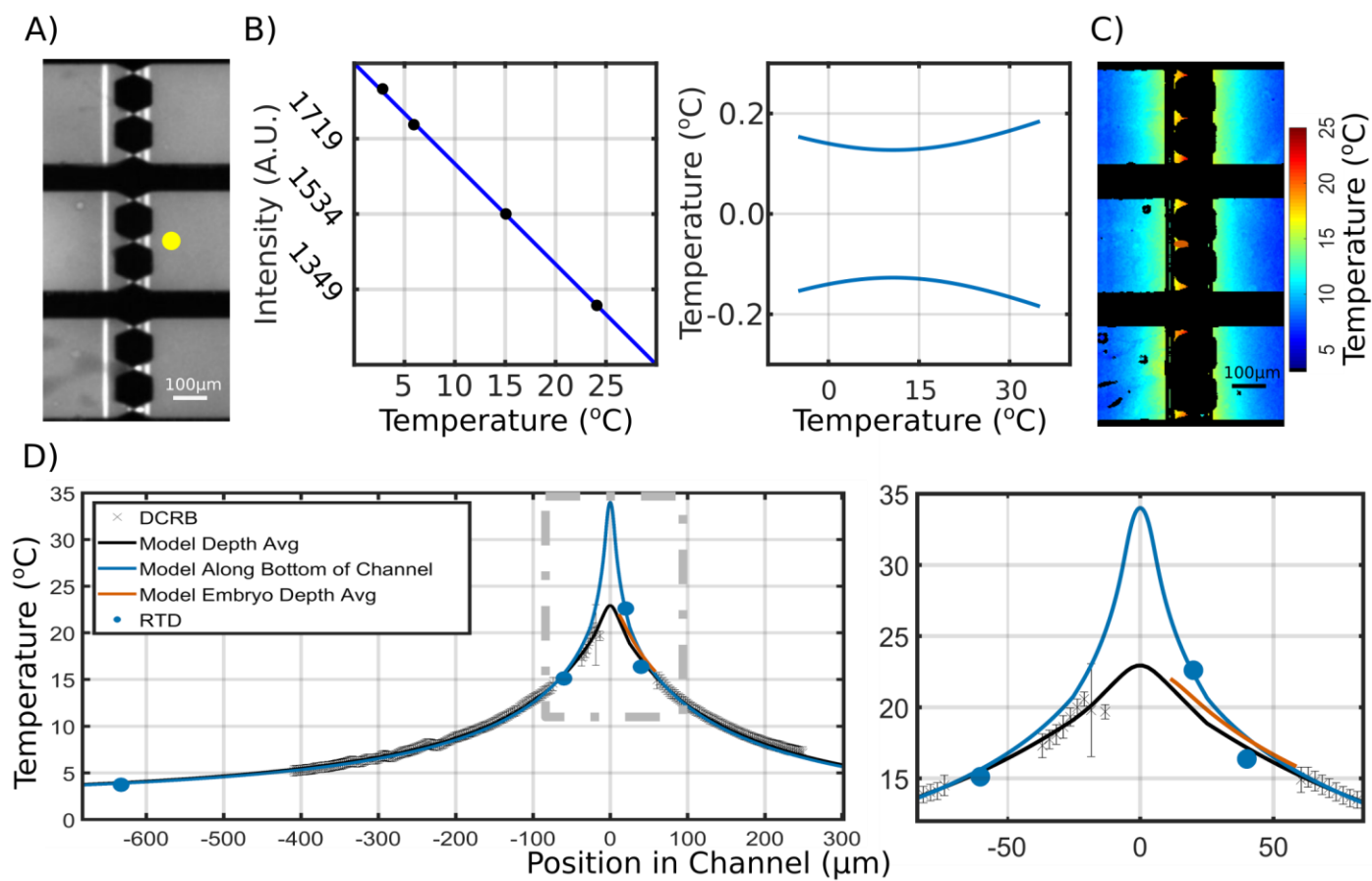
713 posterior cell  $P_1$  at a uniform permissive T. Bottom and middle panels: example of two  
714 embryos experiencing a reversal of the division sequence of AB and  $P_1$ , along with 100X  
715 DIC image of an arrested embryo~ 24 hours after being in T gradient. The embryo had  
716 progressed through morphogenesis and elongation despite the reversed sequence of AB-  
717  $P_1$  divisions.  
718

719 **Figure 1. Microfluidic device design**

720



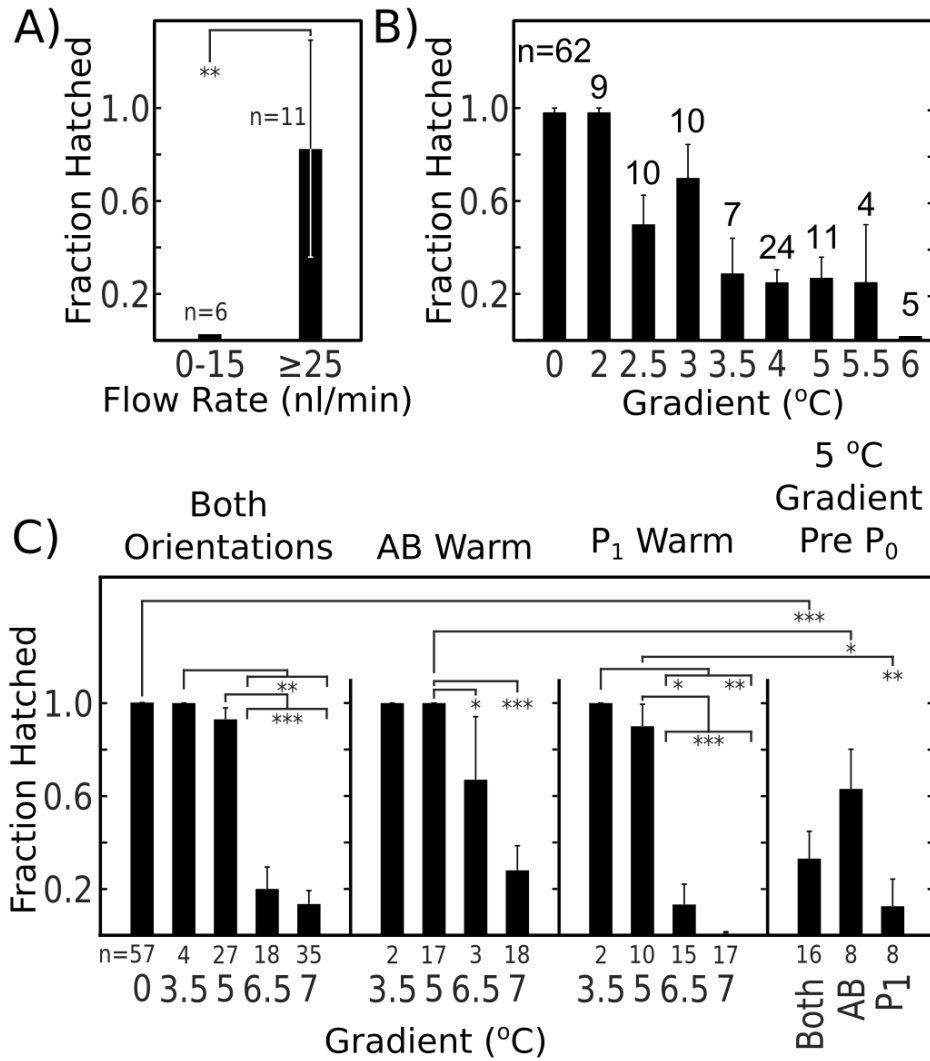
721 **Figure 2. Characterization of the T gradient in the microfluidic device.**



722

723 **Figure 3. Survival in the T gradient is dependent on both the magnitude of the**  
 724 **gradient and orientation of the embryo**

725

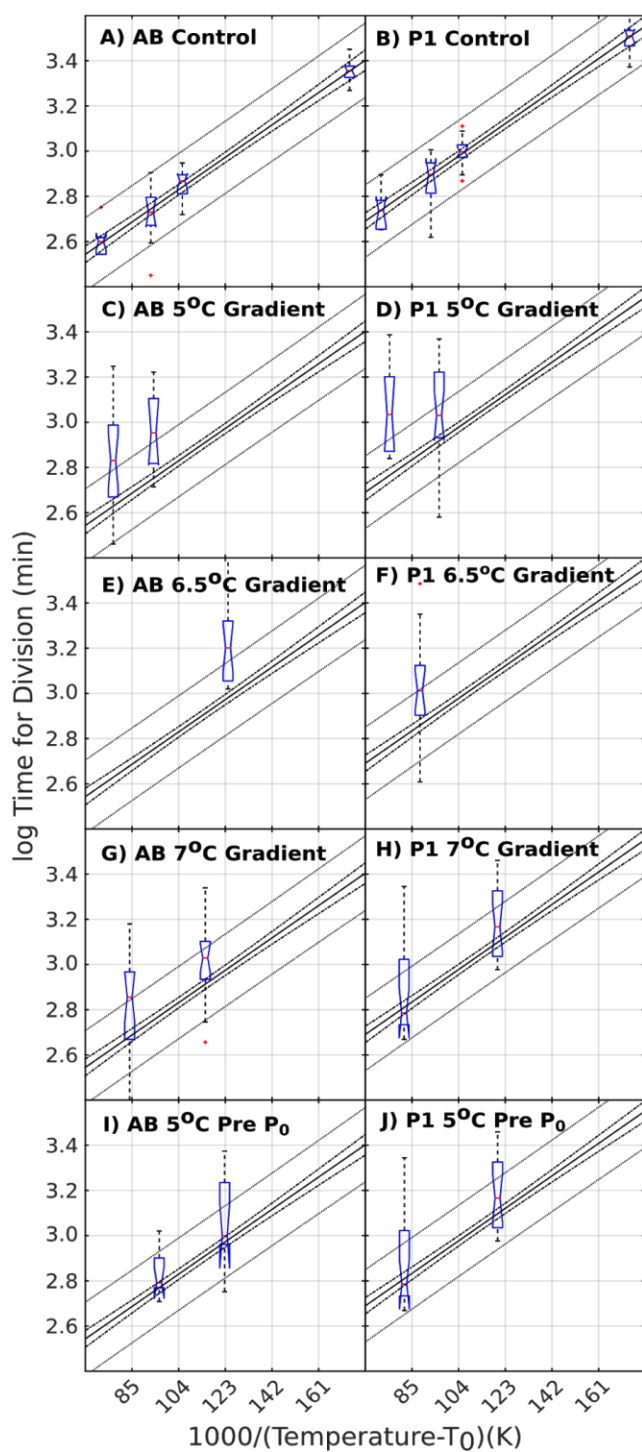


726

727

728  
729

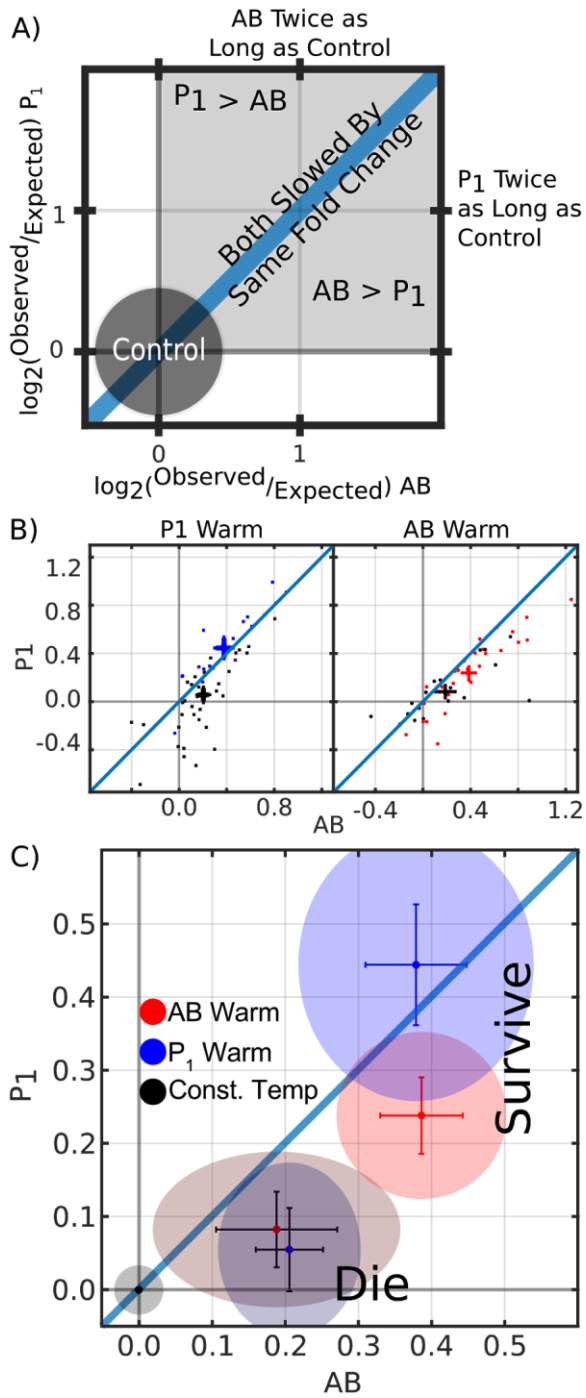
**Figure 4. Cell division rates of individual blastomeres in the T gradient**



730

731 **Figure 5. Analysis of deviations in division rates of AB and P<sub>1</sub>.**

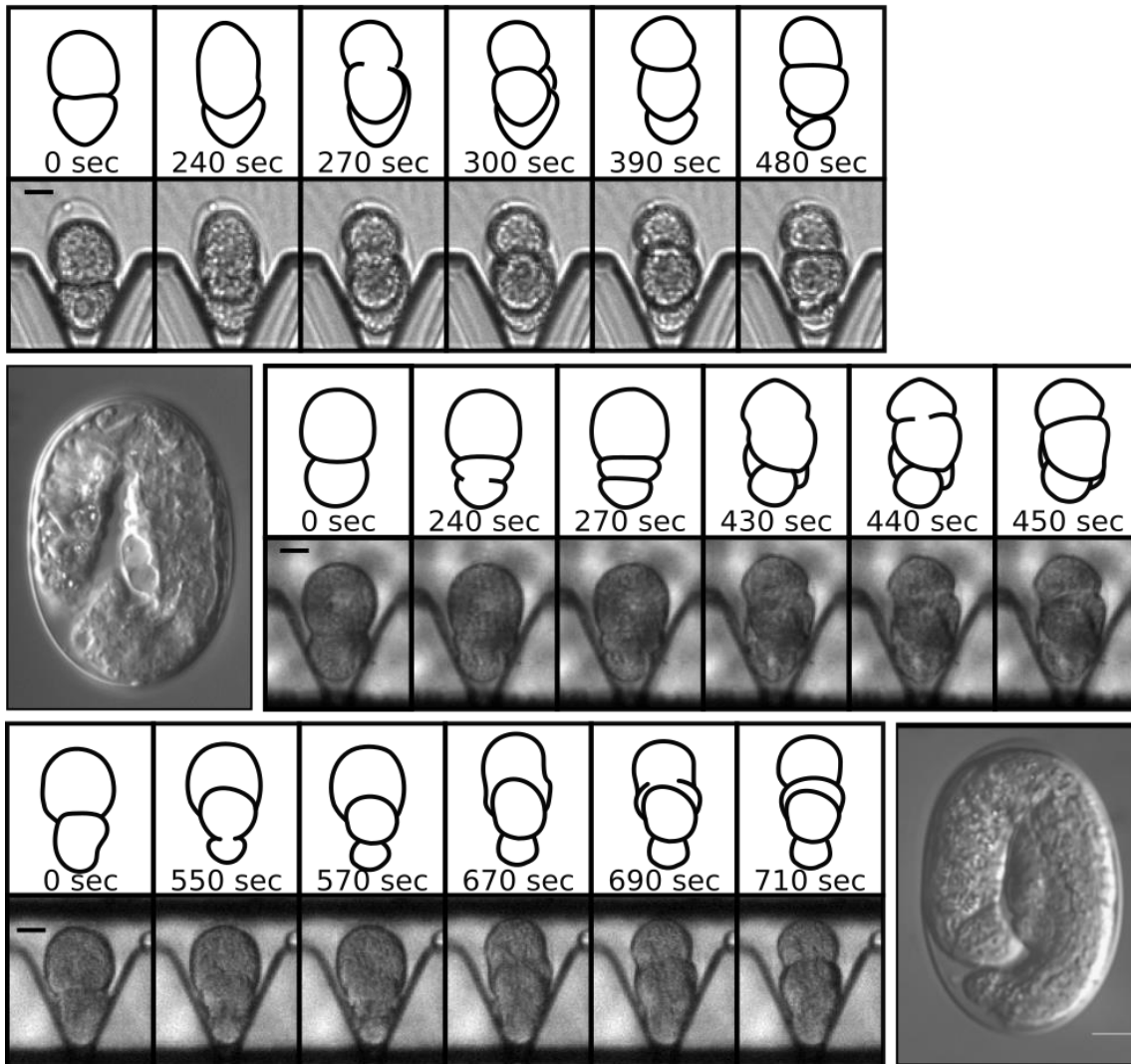
732



733  
734

**Figure 6. Relatively normal morphogenesis following out of sequence divisions of AB and P<sub>1</sub>.**

735





736

- 737 1. Felix MA, Wagner A. Robustness and evolution: concepts, insights and challenges from a  
738 developmental model system. *Hered.* 2008;100: 132–140. doi:10.1038/sj.hdy.6800915
- 739 2. Mantikou E, Wong KM, Repping S, Mastenbroek S. Molecular origin of mitotic aneuploidies  
740 in preimplantation embryos. *Biochimica et Biophysica Acta - Molecular Basis of Disease.*  
741 Elsevier; 2012. pp. 1921–1930. doi:10.1016/j.bbadis.2012.06.013
- 742 3. Houchmandzadeh B, Wieschaus E, Leibler S. Establishment of developmental precision  
743 and proportions in the early *Drosophila* embryo. *Nature.* 2002;415: 798–802.  
744 doi:10.1038/415798a
- 745 4. Barbash-Hazan S, Frumkin T, Malcov M, Yaron Y, Cohen T, Azem F, et al. Preimplantation  
746 aneuploid embryos undergo self-correction in correlation with their developmental  
747 potential. *Fertil Steril.* 2009;92: 890–896. doi:10.1016/j.fertnstert.2008.07.1761
- 748 5. Kosubek A, Klein-Hitpass L, Rademacher K, Horsthemke B, Ryffel GU. Aging of *Xenopus*  
749 *tropicalis* Eggs Leads to Deadenylation of a Specific Set of Maternal mRNAs and Loss of  
750 Developmental Potential. Veenstra GJC, editor. *PLoS One.* 2010;5: e13532.  
751 doi:10.1371/journal.pone.0013532
- 752 6. Wood WB, Hecht R, Carr S, Vanderslice R, Wolf N, Hirsh D. Parental effects and phenotypic  
753 characterization of mutations that affect early development in *Caenorhabditis elegans*.  
754 *Dev Biol.* 1980;74: 446–469.
- 755 7. Ward S, Miwa J. Characterization of temperature-sensitive, fertilization-defective mutants  
756 of the nematode *caenorhabditis elegans*. *Genetics.* 1978;88: 285–303.
- 757 8. Ben-David E, Burga A, Burga A, Kruglyak L. A maternal-effect selfish genetic element in  
758 *Caenorhabditis elegans*. *Science* (80- ). 2017;356: 1051–1055.  
759 doi:10.1126/SCIENCE.AAN0621
- 760 9. Yeyati PL, van Heyningen V. Incapacitating the evolutionary capacitor: Hsp90 modulation  
761 of disease. *Curr Opin Genet Dev.* 2008;18: 264–272. doi:10.1016/j.gde.2008.07.004
- 762 10. Rutherford S, Hirate Y, Swalla BJ. The Hsp90 capacitor, developmental remodeling, and  
763 evolution: the robustness of gene networks and the curious evolvability of  
764 metamorphosis. *Crit Rev Biochem Mol Biol.* 2007;42: 355–372.  
765 doi:10.1080/10409230701597782
- 766 11. Rutherford SL, Lindquist S. Hsp90 as a capacitor for morphological evolution. *Nature.*  
767 1998;396: 336–342. doi:10.1038/24550
- 768 12. Rohner N, Jarosz DF, Kowalko JE, Yoshizawa M, Jeffery WR, Borowsky RL, et al. Cryptic  
769 variation in morphological evolution: HSP90 as a capacitor for loss of eyes in cavefish.  
770 *Science* (80- ). 2013;342: 1372–1375. doi:10.1126/science.1240276
- 771 13. Sollars V, Lu X, Xiao L, Wang X, Garfinkel MD, Ruden DM. Evidence for an epigenetic  
772 mechanism by which Hsp90 acts as a capacitor for morphological evolution. *Nat Genet.*  
773 2003;33: 70–74. doi:10.1038/ng1067
- 774 14. Queitsch C, Sangster TA, Lindquist S. Hsp90 as a capacitor of phenotypic variation. *Nature.*  
775 2002;417: 618–624. doi:10.1038/nature749
- 776 15. Eldar A, Shilo BZ, Barkai N. Elucidating mechanisms underlying robustness of morphogen  
777 gradients. *Current Opinion in Genetics and Development.* Elsevier Current Trends; 2004.  
778 pp. 435–439. doi:10.1016/j.gde.2004.06.009
- 779 16. Cheung D, Miles C, Kreitman M, Ma J. Adaptation of the length scale and amplitude of the

- 780 Bicoid gradient profile to achieve robust patterning in abnormally large *Drosophila*  
781 *melanogaster* embryos. *Dev.* 2014;141: 124–135. doi:10.1242/dev.098640
- 782 17. Jiang YJ, Aerne BL, Smithers L, Haddon C, Ish-Horowicz D, Lewis J. Notch signalling and the  
783 synchronization of the somite segmentation clock. *Nature.* 2000;408: 475–479.  
784 doi:10.1038/35044091
- 785 18. Soza-Ried C, Öztürk E, Ish-Horowicz D, Lewis J. Pulses of Notch activation synchronise  
786 oscillating somite cells and entrain the zebrafish segmentation clock. *Dev.* 2014;141:  
787 1780–1788. doi:10.1242/dev.102111
- 788 19. Oates AC, Morelli LG, Ares S. Patterning embryos with oscillations: Structure, function and  
789 dynamics of the vertebrate segmentation clock. *Development.* Oxford University Press for  
790 The Company of Biologists Limited; 2012. pp. 625–639. doi:10.1242/dev.063735
- 791 20. Sulston JE, White JG, Thomson JN, SE, Sulston JE, Schierenberg E, White JG, Thomson JN. The  
792 embryonic cell lineage of the nematode *Caenorhabditis elegans*. *Developmental Biology*  
793 1983 pp. 64–119. doi:10.1016/0012-1606(83)90201-4
- 794 21. Bao Z, Zhao Z, Boyle TJ, Murray JI, Waterston RH. Control of cell cycle timing during *C.*  
795 *elegans* embryogenesis. *Dev Biol.* 2008/04/24. 2008;318: 65–72. doi:10.1016/j.ydbio.2008.02.054
- 796 22. Priess JR. Notch signaling in the *C. elegans* embryo. *WormBook.* 2005; 1–16.  
797 doi:10.1895/wormbook.1.4.1
- 798 23. Priess JR, Thomson JN. Cellular interactions in early *C. elegans* embryos. *Cell.* 1987;48:  
799 241–250.
- 800 24. Deppe U, Schierenberg E, Cole T, Krieg C, Schmitt D, Yoder B, et al. Cell lineages of the  
801 embryo of the nematode *Caenorhabditis elegans*. *Proc Natl Acad Sci U S A.* 1978;75: 376–  
802 380.
- 803 25. Schierenberg E, Wood WB. Control of cell-cycle timing in early embryos of *Caenorhabditis*  
804 *elegans*. *Dev Biol.* 1985;107: 337–354.
- 805 26. Robertson SM, Medina J, Lin R. Uncoupling Different Characteristics of the *C. elegans* E  
806 Lineage from Differentiation of Intestinal Markers. Goldstein B, editor. *PLoS One.* 2014;9:  
807 e106309. doi:10.1371/journal.pone.0106309
- 808 27. Edgar LG, Goldstein B. Culture and manipulation of embryonic cells. *Methods Cell Biol.*  
809 107: 151.
- 810 28. Goldstein B. Induction of gut in *Caenorhabditis elegans* embryos. *Nature.* 1992;357: 255–  
811 257.
- 812 29. Brauchle M, Baumer K, Gönczy P. Differential activation of the DNA replication checkpoint  
813 contributes to asynchrony of cell division in *C. elegans* embryos. *Curr Biol.* 2003;13: 819–  
814 827. doi:10.1016/S
- 815 30. Arata Y, Takagi H, Sako Y, Sawa H. Power law relationship between cell cycle duration and  
816 cell volume in the early embryonic development of *Caenorhabditis elegans*. *Front Physiol.*  
817 2015;5: 529. doi:10.3389/fphys.2014.00529
- 818 31. Sawa H. Control of cell polarity and asymmetric division in *C. elegans*. *Curr Top Dev Biol.*  
819 2012/11/13. 2012;101: 55–76. doi:10.1016/b978-0-12-394592-1.00003-x
- 820 32. Rose L, Gönczy P. Polarity establishment, asymmetric division and segregation of fate  
821 determinants in early *C. elegans* embryos. *WormBook.* 2014; 1–43.  
822 doi:10.1895/wormbook.1.30.2
- 823

- 824 33. Gonczy P, Rose LS. Asymmetric cell division and axis formation in the embryo. *WormBook*.  
825 2005; 1–20. doi:10.1895/wormbook.1.30.1
- 826 34. Francklyn CS. DNA polymerases and aminoacyl-tRNA synthetases: shared mechanisms for  
827 ensuring the fidelity of gene expression. *Biochemistry*. 2008;47: 11695–11703.  
828 doi:10.1021/bi801500z
- 829 35. Ganai RA, Johansson E. DNA Replication-A Matter of Fidelity. *Mol Cell*. 2016/06/04.  
830 2016;62: 745–755. doi:10.1016/j.molcel.2016.05.003
- 831 36. Wang Y, Badea T, Nathans J. Order from disorder: Self-organization in mammalian hair  
832 patterning. *Proc Natl Acad Sci U S A*. 2006;103: 19800–19805.  
833 doi:10.1073/pnas.0609712104
- 834 37. Briscoe J, Small S. Morphogen rules: Design principles of gradient-mediated embryo  
835 patterning. *Development (Cambridge)*. Company of Biologists Ltd; 2015. pp. 3996–4009.  
836 doi:10.1242/dev.129452
- 837 38. Schweisguth F, Corson F. Self-Organization in Pattern Formation. *Developmental Cell*. Cell  
838 Press; 2019. pp. 659–677. doi:10.1016/j.devcel.2019.05.019
- 839 39. Martinez Arias A, Steventon B. On the nature and function of organizers. *Development*  
840 (Cambridge). Company of Biologists Ltd; 2018. doi:10.1242/dev.159525
- 841 40. Tautz D. Redundancies, development and the flow of information. *BioEssays*. 1992;14:  
842 263–266. doi:10.1002/bies.950140410
- 843 41. Zhang Z, Zwick S, Loew E, Grimley JS, Ramanathan S. Mouse embryo geometry drives  
844 formation of robust signaling gradients through receptor localization. *Nat Commun*.  
845 2019;10: 1–14. doi:10.1038/s41467-019-12533-7
- 846 42. Akieda Y, Ogamino S, Furuie H, Ishitani S, Akiyoshi R, Nogami J, et al. Cell competition  
847 corrects noisy Wnt morphogen gradients to achieve robust patterning in the zebrafish  
848 embryo. *Nat Commun*. 2019;10: 1–17. doi:10.1038/s41467-019-12609-4
- 849 43. Averbukh I, Lai SL, Doe CQ, Barkai N. A repressor-decay timer for robust temporal  
850 patterning in embryonic drosophila neuroblast lineages. *Elife*. 2018;7.  
851 doi:10.7554/eLife.38631
- 852 44. Niemuth J, Wolf R. Developmental asynchrony caused by steep temperature gradients  
853 does not impair pattern formation in the wasp, *Pimpla turionellae* L. *Roux Arch Dev Biol*.  
854 1995/08/01. 1995;204: 444–452. doi:10.1007/bf00360852
- 855 45. Lucchetta EM, Lee JH, Fu LA, Patel NH, Ismagilov RF. Dynamics of *Drosophila* embryonic  
856 patterning network perturbed in space and time using microfluidics. *Nature*. 2005/04/29.  
857 2005;434: 1134–1138. doi:10.1038/nature03509
- 858 46. Richards JL, Zacharias AL, Walton T, Burdick JT, Murray JI. A quantitative model of normal  
859 *Caenorhabditis elegans* embryogenesis and its disruption after stress. *Dev Biol*. 2013;374:  
860 12–23. doi:10.1016/j.ydbio.2012.11.034
- 861 47. Zacharias AL, Murray JI. Combinatorial decoding of the invariant *C. elegans* embryonic  
862 lineage in space and time. *Genesis*. 2016;54: 182–197. doi:10.1002/dvg.22928
- 863 48. Byerly L, Cassada RC, Russell RL. The life cycle of the nematode *Caenorhabditis elegans*. I.  
864 Wild-type growth and reproduction. *Dev Biol*. 1976;51: 23–33. doi:10.1016/0012-  
865 1606(76)90119-6
- 866 49. Folkmann AW, Seydoux G. Spatial regulation of the polarity kinase PAR-1 by parallel  
867 inhibitory mechanisms. 2019; doi:10.1242/dev.171116

- 868 50. Singh D, Pohl C. Coupling of rotational cortical flow, asymmetric midbody positioning, and  
869 spindle rotation mediates dorsoventral axis formation in *C. elegans*. *Dev Cell*. 2014;28:  
870 253–267. doi:10.1016/j.devcel.2014.01.002
- 871 51. Elegans C, Briggsae Graphical C, Begasse ML, Grill SW, Hyman AA, Leaver M, et al.  
872 Temperature Dependence of Cell Division Timing Accounts for a Shift in the Thermal Limits  
873 of Temperature Dependence of Cell Division Timing Accounts for a Shift in the Thermal  
874 Limits of *C. elegans* and *C. briggsae*. *Cell Rep*. 2015;10: 647–653.  
875 doi:10.1016/j.celrep.2015.01.006
- 876 52. Nakamura K, Takayanagi T, Sato S. A modified arrhenius equation. *Chem Phys Lett*.  
877 1989;160: 295–298. doi:10.1016/0009-2614(89)87599-2
- 878 53. Motoyama N, Naka K. DNA damage tumor suppressor genes and genomic instability. *Curr*  
879 *Opin Genet Dev*. 2004;14: 11–16. Available:  
880 [http://www.ncbi.nlm.nih.gov/entrez/query.fcgi?cmd=Retrieve&db=PubMed&dopt=Citation&list\\_uids=15108799](http://www.ncbi.nlm.nih.gov/entrez/query.fcgi?cmd=Retrieve&db=PubMed&dopt=Citation&list_uids=15108799)  
881
- 882 54. O’Neil N, Rose A. DNA repair. *WormBook*. 2006; 1–12. doi:10.1895/wormbook.1.54.1
- 883 55. Kastan MB, Bartek J. Cell-cycle checkpoints and cancer. *Nature*. 2004;432: 316–323.  
884 Available:  
885 [http://www.ncbi.nlm.nih.gov/entrez/query.fcgi?cmd=Retrieve&db=PubMed&dopt=Citation&list\\_uids=15549093](http://www.ncbi.nlm.nih.gov/entrez/query.fcgi?cmd=Retrieve&db=PubMed&dopt=Citation&list_uids=15549093)  
886
- 887 56. Gendreau S, Moskowitz IPG, Terns RM, Rothman JH. The Potential to Differentiate  
888 Epidermis is Unequally Distributed in the AB Lineage. *Dev Biol*. 1994;  
889 doi:10.1006/dbio.1994.1355
- 890 57. Djabrayan NJ, Dudley NR, Sommermann EM, Rothman JH. Essential role for Notch signaling  
891 in restricting developmental plasticity. *Genes Dev*. 2012/11/06. 2012;26: 2386–2391.  
892 doi:10.1101/gad.199588.112
- 893 58. Boyle MJ, Seaver EC. Developmental expression of foxA and gata genes during gut  
894 formation in the polychaete annelid, *Capitella* sp. I. *Evol Dev*. 2008;10: 89–105.  
895 doi:10.1111/j.1525-142X.2007.00216.x
- 896 59. Edgar LG, McGhee JD. Embryonic expression of a gut-specific esterase in *Caenorhabditis*  
897 *elegans*. *Dev Biol*. 1986;114: 109–118.
- 898 60. Maduro MF. Gut development in *C. elegans*. *Semin Cell Dev Biol*. 2017;66: 3–11.  
899 doi:<https://doi.org/10.1016/j.semcdb.2017.01.001>
- 900 61. Moskowitz IP, Gendreau SB, Rothman JH, Ivan P. G. Moskowitz, Steven B. Gendreau, Joel  
901 H. Rothman. Combinatorial specification of blastomere identity by glp-1-dependent  
902 cellular interactions in the nematode *Caenorhabditis elegans*. *Development*. 1994;120:  
903 3325–3338. Available: <http://dev.biologists.org/content/develop/120/11/3325.full.pdf>
- 904 62. Tax FE, Thomas JH. Cell-cell interactions. Receiving signals in the nematode embryo. *Curr*  
905 *Biol*. 1994;4: 914–916.
- 906 63. Mello CC, Draper BW, Priess JR. The maternal genes apx-1 and glp-1 and establishment of  
907 dorsal-ventral polarity in the early *C. elegans* embryo. *Cell*. 1994;77: 95–106.
- 908 64. Sawa H, Korswagen HC. Wnt signaling in *C. elegans*. *WormBook*. 2013; 1–30.  
909 doi:10.1895/wormbook.1.7.2
- 910 65. Bao Z, Murray JI, Boyle T, Ooi SL, Sandel MJ, Waterston RH. Automated cell lineage tracing  
911 in *Caenorhabditis elegans*. *Proc Natl Acad Sci U S A*. 2006/02/16. 2006;103: 2707–2712.

- 912 doi:0511111103 [pii]10.1073/pnas.0511111103
- 913 66. Schnabel R, Hutter H, Moerman D, Schnabel H. Assessing normal embryogenesis in  
914 *Caenorhabditis elegans* using a 4D microscope: variability of development and regional  
915 specification. *Dev Biol.* 1997;184: 234–265. doi:10.1006/dbio.1997.8509
- 916 67. Budirahardja Y, Gonczy P. PLK-1 asymmetry contributes to asynchronous cell division of *C.*  
917 *elegans* embryos. *Development.* 2008;135: 1303–1313. doi:10.1242/dev.019075
- 918 68. Rivers DM, Moreno S, Abraham M, Ahringer J. PAR proteins direct asymmetry of the cell  
919 cycle regulators Polo-like kinase and Cdc25. *J Cell Biol.* 2008;180: 877–885.  
920 doi:10.1083/jcb.200710018
- 921 69. Wei Y, Multi S, Yang C-R, Ma J, Zhang Q-H, Wang Z-B, et al. Spindle Assembly Checkpoint  
922 Regulates Mitotic Cell Cycle Progression during Preimplantation Embryo Development.  
923 Wang H, editor. *PLoS One.* 2011;6: e21557. doi:10.1371/journal.pone.0021557
- 924 70. Artus J, Cohen-Tannoudji M. Cell cycle regulation during early mouse embryogenesis. *Mol*  
925 *Cell Endocrinol.* 2008;282: 78–86. doi:10.1016/j.mce.2007.11.008
- 926 71. Clute P, Masui Y. Microtubule Dependence of Chromosome Cycles in *Xenopus*  
927 *laevis* Blastomeres under the Influence of a DNA Synthesis Inhibitor, Aphidicolin. *Dev Biol.*  
928 1997;185: 1–13. doi:10.1006/dbio.1997.8540
- 929 72. Ikegami R, Rivera-Bennetts AK, Brooker DL, Yager TD. Effect of inhibitors of DNA replication  
930 on early zebrafish embryos: evidence for coordinate activation of multiple intrinsic cell-  
931 cycle checkpoints at the mid-blastula transition. *Zygote.* 1997;5: 153–175. Available:  
932 <http://www.ncbi.nlm.nih.gov/pubmed/9276512>
- 933 73. Pourquié O. Vertebrate Somitogenesis. *Annu Rev Cell Dev Biol.* 2001;17: 311–350.  
934 doi:10.1146/annurev.cellbio.17.1.311
- 935 74. Greenwald I. LIN-12/Notch signaling in *C. elegans*. *WormBook.* 2005; 1–16.  
936 doi:10.1895/wormbook.1.10.1
- 937 75. Moskowitz IP, Rothman JH. lin-12 and glp-1 are required zygotically for early embryonic  
938 cellular interactions and are regulated by maternal GLP-1 signaling in *C. elegans*.  
939 *Development.* 1996;122: 4105–4117.
- 940 76. Hashimshony T, Feder M, Levin M, Hall BK, Yanai I. Spatiotemporal transcriptomics reveals  
941 the evolutionary history of the endoderm germ layer. *Nature.* 2015;519: 219–222.  
942 doi:10.1038/nature13996
- 943 77. Levin M, Hashimshony T, Wagner F, Yanai I. Developmental milestones punctuate gene  
944 expression in the *Caenorhabditis* embryo. *Dev Cell.* 2012/05/09. 2012;22: 1101–1108.  
945 doi:S1534-5807(12)00142-6 [pii]10.1016/j.devcel.2012.04.004 [doi]
- 946 78. Kuntz SG, Eisen MB, Lerat E, Vieira C, Carareto C. *Drosophila* Embryogenesis Scales  
947 Uniformly across Temperature in Developmentally Diverse Species. Desplan C, editor. *PLoS*  
948 *Genet.* 2014;10: e1004293. doi:10.1371/journal.pgen.1004293
- 949 79. Cruz M, Garrido N, Herrero J, Pérez-Cano I, Muñoz M, Meseguer M. Timing of cell division  
950 in human cleavage-stage embryos is linked with blastocyst formation and quality. *Reprod*  
951 *Biomed Online.* 2012;25: 371–381. doi:10.1016/j.rbmo.2012.06.017
- 952 80. Stiernagle T, Stiernagle T. Maintenance of *C. elegans* [Internet]. 2006 pp. 1–11.  
953 doi:10.1895/wormbook.1.101.1
- 954

## 1 **Supplementary Text**

### 2 **Device construction**

3 The microfluidic device is constructed as two main layers: the backplane, containing the  
4 vias and electrodes of the device and a second layer of microchannels placed on top of  
5 the backplane. Three input and output tapering hemi-conical vias, approximately 2 mm  
6 wide, and 800-900  $\mu\text{m}$  deep at the edge, are made in a 1"x3" commercially available  
7 microscope slide cut in half to 1"x1.5". To prevent impurity migration from the microscope  
8 slide, 100-150 nm of  $\text{SiO}_2$  is reactive sputter deposited on the backplane. Electrodes of  
9 10 nm Ti followed by 100 nm of Pt were patterned on microscope slides using standard  
10 negative photoresist clean room photolithography. The electrode face of the device is  
11 covered with an approximate 2  $\mu\text{m}$  layer of SU-8 2002 (MicroChem Corp., Westborough,  
12 MA). Centered on the device, an  $\sim 1\text{cm}$  diameter and 750-800  $\mu\text{m}$  deep circular cut, under  
13 and in the opposite face of the glass, is HF etched into the glass which allowed a steep T  
14 gradient of  $7.5^\circ\text{C}$  by reducing the thickness of the coverslip and ensuring the heat was  
15 dissipated away by circulation of chilled water. A positive master mold of our microfluidic  
16 channel design was dry etched 40  $\mu\text{m}$  deep into a 3" silicon wafer with a negative PDMS  
17 mold made from the silicon wafer using standard soft lithography techniques [1]. The  
18 microfluidic "sticker" layer of the device is constructed consistent with methods developed  
19 by Bartolo et al. [2], and is placed on top of the electrodes with the capture pillars of the  
20 device centered on the electrodes of the backplane. 0.03" outer diameter PTFE tubing is  
21 inserted into the device vias, and secured with two-part epoxy.

22 Device is mounted on a custom-built device holder/flow cell that allows bulk fluid flow  
23 underneath and in contact with the outside bottom surface of the microfluidic device.

24 Tubing (~0.25" ID PDMS) connects the flow cell to a water circulator filled with DI water  
25 and ethylene glycol in a ratio of 4:1. Flow rate through the fluid cell is on the order of 19  
26 ml/sec. The water circulator is used to set the background T of the device. Device  
27 holder/flow cell and device are loaded into a custom rig on an upright microscope. A  
28 custom environmental chamber enclosing the microscope is maintained at a slight  
29 positive pressure with sub 0°C dew point laboratory supplied air to prevent condensation  
30 on device during operation.

31

### 32 **Characterization of the T gradient**

33 Effect of T on the fluorescence response of Rhodamine B has been extensively studied  
34 and its quantum yield is highly T dependent[3–5]. It has been previously reported that a  
35 solution of dextran-conjugated fluorophores can aggregate, resulting in an apparent  
36 increase in quantum efficiency of the fluorophore, and that the aggregation rate is T  
37 dependent [6]. To address this concern, we performed our measurements with a flow of  
38 the solution running during measurements. To ensure the introduced flow would not affect  
39 the T profile of the device we calculated the expected flow rate of our device for which the  
40  $Pe$  would equal one and found it to be on the order of 1-2 $\mu$ l/min. We then measured the  
41 effect of fluid flow above and below this threshold with thermometric microscopy utilizing  
42 DCRB. We found that a flow of 2 $\mu$ l/min did not affect the T profile of the gradient, while at  
43 flow of 15 $\mu$ l/min shifted the T profile in the direction of flow. In later devices, in addition to  
44 characterization of the T gradient with thermometric microscopy, we also included  
45 resistive thermal sensors or devices (RTDs) [7] in the T gradient region of the device. The  
46 device is placed in a well stirred ice bath and allowed to come up to room T while

47 measuring the T of the bath with thermocouples and resistance of the RTDs. Standard  
48 least squares fitting is used to relate the RTD measurements with T. We found a highly  
49 linear correlation between T and the measured resistance, and modeled the relationship  
50 between the two using a least squares linear model.  $R^2$  values of linear models fitting  
51 resistance to Ts ranging from 0°C to 20°C were typically on the order of 0.999. To verify  
52 that the RTDs were primarily measuring the T in the region of the T gradient, and not the  
53 electrode leads leading up to that region, we measured the resistance of the patterned  
54 RTDs with the device mounted on a flow cell that flowed a fixed and measured T of water  
55 below the region of the device where the T gradient is established. We found that our T  
56 measurements were within 1°C of the experiment in which the device was fully  
57 submerged.

58 During normal operation of the device, the device is not submerged in fluid. To  
59 verify that our T measurement was a reasonable estimate of the T in the channel, and not  
60 just the bottom of the channel, we constructed a modified flow cell that allowed the flow  
61 of the T setting water both underneath as well as over the top of the device. We found  
62 that the average difference in T measured between when the top of the device is exposed  
63 to air, and when it is sandwiched between flowing fluid was on the order of a third of a  
64 degree.

65

### 66 **Modeling the apparent intra-embryonic T gradient.**

67 We modeled the embryo as a 50x30  $\mu\text{m}$  spheroid with thermal conductivity equal to that  
68 of water,  $k_{\text{cytoplasm}}=0.6$  W/m-K [8], and an insulating eggshell of 300 nm thickness [9].  
69 Although cytoplasm is a gel matrix, thermal conductivity of a gel, for example a



70 concentrated protein solution of 10% gelatin, is only 5% lower in conductivity than water  
71 [10]. While thermal conductivity of nematode eggshells has not been measured, a model  
72 of *Drosophila* embryos [8] used  $k_{\text{shell}}=k_{\text{paraffin wax}}=0.25 \text{ W/m-K}$ , 10x more insulating than  
73 an avian eggshell. Using this extreme value in our simulation, the intra-embryonic  
74 gradient was reduced by only 1%. We also considered the possibility that extremely active  
75 fluid circulation within the embryo might overcome the T gradient within the embryo by  
76 convective transport. The Peclet number (Pe) of a system indicates whether convection  
77 or diffusion dominates in determining the distribution of heat. A Pe of one indicates a  
78 system where convection and diffusion are in balance. Values higher than one indicate  
79 convection dominates and values lower than one indicate diffusion dominates. The  
80 maximum known cytoplasmic streaming velocity in the *C. elegans* embryo of  $7 \mu\text{m}/\text{min}$   
81 [11], cannot overcome thermal diffusion at this scale as the Peclet (Pe) number of the  
82 embryo with known dimensions and expected possible highest velocity is only  $2.5 \times 10^{-5}$ .  
83 Thus, the T gradient within the embryo is in close accordance with the external T gradient  
84 in the microfluidic device.

## 85 **Verification that the microfluidic device is compatible with embryonic development**

86 To verify compatibility of the device with embryo development, a cohort of early  
87 stage embryos (1-8 cell stage) were loaded into the device and allowed to develop to  
88 hatching while in the device. Below a certain threshold of flow, the embryos tended to  
89 arrest during development and or not complete development. This finding was consistent  
90 with the material from which the device was constructed, NOA81, being gas impermeable  
91 [12]. Flow rates in excess of  $25 \text{ nl}/\text{min}$  prevented arrest of embryos during development.  
92 Having previously calculated the Pe of the device and measured the effect of fluid flow

93 below the critical rate, we were confident that a flow rate of 100-500nl/min within the  
94 device would not affect the T profile of the device while simultaneously creating a  
95 biologically compatible environment. Our real time RTD measurements of T in the device  
96 in our later experiments also demonstrated that the T profile at these slower flow rates  
97 remained similar to those without flow. To determine the effect of loading and unloading  
98 on the survival of the embryos, we loaded a cohort of one-celled and two-celled embryos  
99 into a room T device at 80 $\mu$ l/min, left them in the device for ~ 1 hour, with a trickling flow  
100 of 500nl/min and unloaded them at a rate of 300 $\mu$ l/min. Each embryo was then placed on  
101 an agar plate and evaluated for whether or not they had successfully developed and  
102 hatched 24 hours later. We found that the rate of hatching was 98.4% (61/62). We were  
103 thus able to optimize the parameters that ensured the viability of the embryos was not  
104 adversely affected in the microfluidic device under control conditions of uniform T.

105

#### 106 **Supplementary movies:**

##### 107 **Movie S1**

108 Animation of fly-over and through of device. All device sizes are approximately to scale  
109 relative to the bulk substrate of the device which has an aspect ratio of 1:3:1/25.4 (aspect  
110 ratio of a typical commercially available microscope slide)

111

##### 112 **Movie S2**

113 High speed camera acquisition of loading of a single embryo were taken at 10k frames  
114 per second at 10x on inverted Nikon Eclipse. Replay speed was 10 frames per second.

115

- 116 1. Xia Y, Whitesides GM. SOFT LITHOGRAPHY. *Annu Rev Mater Sci.* 1998;28: 153–184.  
117 doi:10.1146/annurev.matsci.28.1.153
- 118 2. Bartolo D, Degré G, Nghe P, Studer V. Microfluidic stickers. *Lab Chip.* 2008;8: 274–279.  
119 doi:10.1039/b712368j
- 120 3. Wang XD, Wolfbeis OS, Meier RJ. Luminescent probes and sensors for temperature. *Chem Soc Rev.*  
121 2013;42: 7834–7869. doi:10.1039/c3cs60102a
- 122 4. Ross D, Gaitan M, Locascio LE. Temperature measurement in microfluidic systems using a  
123 temperature-dependent fluorescent dye. *Anal Chem.* 2001;73: 4117–4123.  
124 doi:10.1021/ac010370l
- 125 5. Glawdel T, Almutairi Z, Wang S, Ren C. Photobleaching absorbed Rhodamine B to improve  
126 temperature measurements in PDMS microchannels. 2009/02/12. 2009;9: 171–174.  
127 doi:10.1039/b805172k
- 128 6. Filippov SK, Lezov A V., Sergeeva OY, Olifirenko AS, Lesnichin SB, Domnina NS, et al. Aggregation of  
129 dextran hydrophobically modified by sterically-hindered phenols in aqueous solutions: Aggregates  
130 vs. single molecules. *Eur Polym J.* 2008;44: 3361–3369. doi:10.1016/j.eurpolymj.2008.07.041
- 131 7. Bolker BFT, Sidles PH. Thin-film platinum resistance thermometers: Fabrication and use. *J Vac Sci  
132 Technol.* 1977;14: 205–209. doi:10.1116/1.569123
- 133 8. Lucchetta EM, Lee JH, Fu LA, Patel NH, Ismagilov RF. Dynamics of *Drosophila* embryonic patterning  
134 network perturbed in space and time using microfluidics. *Nature.* 2005/04/29. 2005;434: 1134–  
135 1138. doi:10.1038/nature03509
- 136 9. Johnston WL, Dennis JW. The eggshell in the *C. elegans* oocyte-to-embryo transition. *genesis.*  
137 2012;50: 333–349. doi:10.1002/dvg.20823
- 138 10. Boggs J, Sibbitt W. Thermal Conductivity Measurements of Viscous Liquids. *Ind Eng Chem.* 1955;47:  
139 53. doi:10.1021/ie50542a611
- 140 11. Hird SN, White JG. Cortical and cytoplasmic flow polarity in early embryonic cells of *Caenorhabditis  
141 elegans.* *J Cell Biol.* 1993;121: 1343–1355.
- 142 12. Bong KW, Xu J, Kim J-H, Chapin SC, Strano MS, Gleason KK, et al. Non-polydimethylsiloxane devices  
143 for oxygen-free flow lithography. *Nat Commun.* 2012;3: 805. doi:10.1038/ncomms1800

144  
145